International Journal of Nanomedicine

Dovepress
open access to scientific and medical research

Open Access Full Text Article

ORIGINAL RESEARCH

Comparative Toxicological Effects of Biologically and Chemically Synthesized Copper Oxide Nanoparticles on Mice

This article was published in the following Dove Press journal:
International Journal of Nanomedicine

Badr E El Bialy [1]
Ragaa A Hamouda [2,3]
Mabrouk A Abd Eldaim [4]
Salah S El Ballal [5]
Hanim S Heikal [6]
Hanem K Khalifa [7]
Wael N Hozzein [8,9]

[1]Department of Forensic Medicine and Toxicology, Faculty of Veterinary Medicine, University of Sadat City, Sadat City, Egypt; [2]Department of Biology, Faculty of Sciences and Arts-Khulais, University of Jeddah, Jeddah, Saudi Arabia; [3]Department of Microbial Biotechnology, Genetic Engineering & Research Institute, University of Sadat City, Sadat City, Egypt; [4]Department of Biochemistry and Chemistry of Nutrition, Faculty of Veterinary Medicine, Menoufia University, Sheben Elkom 32511, Egypt; [5]Department of Pathology, Faculty of Veterinary Medicine, University of Sadat City, Sadat City, Egypt; [6]Department of Animal Husbandry and Animal Wealth Development, Faculty of Veterinary Medicine, University of Sadat City, Sadat City, Egypt; [7]Department of Biochemistry and Chemistry of Nutrition, Faculty of Veterinary Medicine, University of Sadat City, Sadat City, Egypt; [8]Bioproducts Research Chair, Zoology Department, College of Science, King Saud University, Riyadh, Saudi Arabia; [9]Botany and Microbiology Department, Faculty of Science, Beni-Suef University, Beni-Suef, Egypt

Correspondence: Mabrouk A Abd Eldaim
Department of Biochemistry and Chemistry of Nutrition, Faculty of Veterinary Medicine, Menoufia University, Sheben Elkom 32511, Egypt
Tel/Fax +20482193756; +201117484718
Email mabroukattia@vet.menofia.edu.eg

Wael N Hozzein
Bioproducts Research Chair, Zoology Department, College of Science, King Saud University, Sheben Riyadh, Saudi Arabia
Email whozzein@ksu.edu.sa

Introduction: Copper oxide nanoparticles (CuO-NPs) are widely used as feed additives for livestock and poultry and implicated in many biomedical applications; however, overload of copper NPs induces various toxicological changes and dysfunction of animal's organs. Thus, this study was designed to evaluate the comparative toxicological effects of biologically and chemically synthesized CuO-NPs on mice.

Methods: Transmission electron microscopy (TEM), X-ray diffraction (XRD) and Fourier-transform infrared spectroscopy (FT-IR) were used to characterize the sizes, shapes and functional groups of CuO-NPs. Forty-five mice were randomly allocated into three groups. Control group received distilled water. The second group was administered a single dose of biologically synthesized CuO-NPs (500 mg/kg bw) orally. The third group was administered a single dose of chemically synthesized CuO-NPs (500 mg/kg bw) orally.

Results: TEM revealed that biologically synthesized NPs were spherical in shape, whereas chemically synthesized NPs were spherical or elongated in shape. XRD showed that the size of biologically synthesized NPs ranged from 4.14 to 12.82 nm and that of chemically synthesized NPs ranged from 4.06 to 26.82 nm. FT-IR spectroscopy indicated that the peaks appeared between 779 cm^{-1} and 425 cm^{-1} in biologically synthesized NPs and between 858 cm^{-1} and 524 cm^{-1} in chemically synthesized NPs were for Cu-O nanostructure. Four mice died due to administration of biologically synthesized CuO-NPs. Both biologically and chemically synthesized CuO-NPs induced leukocytosis, elevated serum activities of alanine aminotransferase and aspartate aminotransferase and serum levels of urea and creatinine and increased P53 mRNA and caspase-3 protein expressions in hepatic tissues. Moreover, CuO-NPs induced degenerative and necrotized changes in hepatic, renal and splenic tissues. Biochemical, apoptotic and pathological changes were more serious in mice administered with biologically synthesized CuO-NPs.

Conclusion: This study indicated that a high dose of biologically and chemically synthesized CuO-NPs induced adverse effects on hepatic, renal and splenic tissues. At the same dose level, the biologically synthesized CuO-NPs evoked more potent toxic effects than the chemically synthesized CuO-NPs.

Keywords: biologically synthesized CuO-NPs, chemically synthesized CuO-NPs, P53, caspase

Introduction

Nanomaterials are chemicals generally ranging in size from 1 to 100 nm. They have many applications including, electronics, energy production, industries and environmental protection. These applications for nanomaterials are due to their tiny size

and unique properties such as thermal, optical, mechanical, magnetic, and electrical and electron configuration density.[1,2] In addition, nanomaterials are implicated in nanomedicine as antimicrobial agents against many pathogens[3] and as novel drug delivery systems to enhance the performance of medical substances.[4] Furthermore, they enter in diagnostic-imaging materials; cosmetics, sunscreens, coatings, batteries, fuel additives, paints, pigments, tires and cement.[2,5] Widespread use of nanomaterials increases environmental contamination and human exposure to them via several routes such as inhalation, dermal and oral. Their potential toxicity is mainly due to occupational exposure to nanoparticle-containing products and nanotechnology-based therapeutics and diagnostics agents.[6] Utilization of nanomaterials in various applications and their characteristic physical and chemical properties influence their toxicological behavior in vivo by making them interact with biological systems easily and facilitate their cellular uptake and distribution in the body compared with bulk chemicals.[7,8] The nanosize of these particles is likely to increase their toxic effects on mammals and the environment.[1]

Copper nanoparticles (Cu-NPs) and copper oxide nanoparticles (CuO-NPs) are widely used as feed additives for livestock and poultry and production of polymers/plastics and lubricants for metallic coating.[9,10] The excellent thermophysical characteristics of Cu-NPs give them value for applications in the field of electronics technology, such as semiconductors, electronic chips, metal catalyst and heat transfer nanofluids.[10,11] Moreover, they have potent antimicrobial activity against a wide range of disease-causing microorganisms and other nanoparticles are used as an alternative antimicrobial agent in many biomedical applications.[12,13] Cu-NPs, like other nanomaterials, access the environment and the human body through many sources, such as effluents, spills during shipping and administration and consumer products and disposal.[14] Excess exposures to Cu or CuO-NPs have severe and dramatic adverse effects on the biological system.

Recently, it has been indicated that overload of CuO-NPs and Cu-NPs can induce gastrointestinal, hepatic, renal, neuronal and splenic toxicities in rats through generation of reactive oxygen species (ROS) and depletion of antioxidants.[15–17] Oxidative stress caused by Cu-NPs is always accompanied with inflammation and adverse effects on drug metabolism in the liver through inhibition of various CYP450 enzymes expression, which increases the risk of drug-drug interactions in animals.[18]

Physical and chemical methods used for synthesis of nanoparticles have drawbacks such as high cost of production, high energy requirement, and generation of toxic by-products. The new strategies were directed toward the biological methods for synthesis of NPs to overcome the drawbacks of chemical methods. The biological methods are effective, nontoxic, and ecofriendly.[19,20] The biomolecules present in the algal extract and other natural sources including, plants and bacteria have been exploited for NP synthesis[21,22] because plant extracts contain bioactive molecules such as phenols, lipids, carbohydrates, enzymes and proteins that can endow effective antimicrobial activities to the green synthetized NPs.[20] In addition, the available functional groups and enzymes in the algal cell walls act as reducing agents employed for reduction and fabrication of metal and metal oxide NPs at ambient conditions.[23,24]

Although the biologically synthesized Cu-NPs have higher antibacterial activity and higher stability than chemically synthesized Cu-NPs,[25] to the best of our knowledge, studies concerning the toxicities of biologically and chemically synthesized CuO-NPs, especially in mammals, are scarce. Therefore, this study was designed to evaluate the comparative toxicological effects of biologically and chemically synthesized CuO-NPs in mature mice.

Materials and Methods

Chemicals and Kits

Chemicals used for synthesis of CuO-NPs and pathological and immunohistochemical investigations were purchased from Sigma-Aldrich Co. (St Louis, MO, USA) and all were of analytical grade.

Diagnostic kits used for assaying the activities of serum alanine aminotransferase (ALT) and aspartate aminotransferase (AST) and serum levels of urea and creatinine were purchased from Biodiagnostic Company, Egypt. Kits used for determination of P53 mRNA expression in hepatic tissue were purchased from Biovision Company, Egypt.

Synthesis of CuO-NPs

Biological Synthesis of CuO-NPs

CuO-NPs were biologically synthesized by using *Ulva fasciata* (macro green alga) that was collected from shallow water beside Abo-Qir shore, Alexandria, Egypt and identified morphologically according to Taylor.[26] The alga aqueous extract was prepared by adding 1 g of air-dried alga to 100 mL double distilled water (DDW), boiled for 1

h and then filtered. The filtrate was completed to 100 mL by adding DDW.

The biological synthesis of CuO-NPs by using alga aqueous extract was performed according to Abboud et al[27] with slight modification. Briefly, 10 mL of the above-mentioned extract was added to 90 mL DDW containing 2.4 g copper sulfate with continuous stirring for 24 h. Then the solution was centrifuged at 10,000 rpm for 15 min, the supernatant was discarded and the pellet of nanoparticles was collected, dispersed in DDW and centrifuged again to remove any unwanted biological materials. Finally, the obtained CuO-NPs were dried in a hot air oven.

Chemical Synthesis of CuO-NPs

Chemical synthesis of CuO-NPs was performed according the method described by Kahn et al[28] in which copper sulfate pentahydrate ($CuSO_4.5H_2O$) was used as a precursor salt and starch was used as a capping agent for chemical reduction process. Briefly, 120 mL of 0.1 M $CuSO_4.5H_2O$ solution was added to 1.2% starch solution with vigorous stirring for 30 min, and 50 mL of 0.2 M ascorbic acid solution (reducing agent) were added with continuous and rapid stirring. Subsequently, 30 mL of 1 M sodium hydroxide solution were slowly added to the solution with constant stirring and heating at 80°C until solution color turned from yellow to ocher (yellowish orange). After that the solution was cooled and settled overnight. Then the supernatant was carefully discarded and the precipitate was separated by filtration and washed three times with deionized water and ethanol to remove the excess starch that bound with the nanoparticles. Finally the precipitate was dried at room temperature and stored for further analysis and characterization.

Characterization of CuO-NPs

Transmission Electron Microscopy (TEM)

Transmission electron microscopy (TEM; JEOL-2100, Tokyo, Japan) at 120 kV of accelerating voltage was used to characterize the sizes and shapes of both biologically and chemically synthesized CuO-NPs.

X-Ray Diffraction (XRD)

X-ray diffraction (JED-2300T) was used to study nondestructively, the crystallographic structure, physical properties and chemical structure of CuO-NPs.[29,30]

Fourier-Transform Infrared spectroscopy (FT-IR)

Fourier-transform infrared spectroscopy was used to investigate the structural and conformational changes of the coordinating self-assembled functional groups on the surface of CuO-NPs. FT-IR spectrometer (FT-IR-6100 type A, Nicolete IS10, Thermo Fisher Scientific, Waltham, MA, USA) of the sample was occupied in the region between 4000 and 400 cm^{-1}.

Acute Toxicological Studies

Animals

Forty-five healthy mature male mice (30–35 g) were obtained from the Department of Husbandry and Animal Wealth Development, Faculty of Veterinary Medicine, University of Sadat City, Egypt. The mice were housed in mouse-specific polypropylene cages (five mice in each cage) and kept in a clean well-ventilated animal room (21 ±3°C, 45–60% RH, natural light/dark cycle) and provided with a standard commercial diet and clean tap water ad libitum. Mice were acclimatized to these environmental conditions for 10 days prior to the beginning of the experiment. This study was ethically approved by the International Animal Care and Use Committee IACUC, following the guidelines of the care and use of laboratory animals, Faculty of Veterinary Medicine, University of Sadat City, Egypt, which follow the Guide for the Care and Use of Laboratory Animals 8th edition. Washington (DC): National Academies Press (US); 2011.

Experimental Design

The mice were randomly allocated into three groups, 15 mice in each:

Control group was given distilled water (0.2 mL/animal) orally.

The biological CuO-NPs group was administered a single dose of biologically synthesized CuO-NPs at a dose of 500 mg/kg bw, dissolved in distilled water (0.2 mL/animal) orally according to Chen et al.[31]

The chemical CuO-NPs group was administrated a single dose of chemically synthesized CuO-NPs at a dose of 500 mg/kg bw, dissolved in distilled water (0.2 mL/animal) orally according to Chen et al.[31]

The calculated dose of each form of Cu-NPs according to the weight and number of mice was freshly prepared by suspending NPs in distilled water using an Ultrasonic homogenizer sonicator on ice media for 10 mins (BioLogics Inc., Manassas, VA USA).

Samples Collection

Forty-eight hours following administration of CuO-NPs, all mice were anesthetized by using isoflurane inhalation. Blood samples were collected by cardiac puncture. Sera samples were separated and kept at −20°C till biochemical assays.

After euthanization of mice, tissue specimens from liver, kidneys, and spleen were excised. One part of each liver was kept at −80°C for evaluation of P53 gene expression. The other part of liver, kidneys and spleen were kept in 10% neutral buffer formalin solution for histopathological and immunohistochemical investigations.

Hematological Assessment

Blood indices including, red blood cell count (RBC), hemoglobin concentration (HGB) and hematocrit percentage (HCT), total leukocytes (TLC) and differential leukocyte counts were estimated by using H32 VET 3-Part Differential Hematology Analyzer (Avantor Performance Materials Inc. Company, Center Valley, PA, USA).

Estimation of Serum Hepatic and Renal Function Biomarkers

The activities of serum ALT and AST were analyzed according to Reitman and Frankel.[32] Serum levels of both urea and creatinine were analyzed according to, Fawcett and Scott[33] and Schirmeister,[34] respectively by using commercial kits following the manufacturer's instructions.

Estimation of Apoptotic Biomarkers

P53 Gene Expression in Hepatic Tissue

Total RNA was isolated from hepatic tissues by using triazole reagent according to manufacturer's instructions and subsequent cDNA was synthesized by using power first strand cDNA synthesis kits, according to the manufacturer protocol. The cDNA that was reverse-transcribed from RNA was used as a template for RT-qPCR. The oligonucleotide primers for P53 were forward primer 5′ GTG GAT CCT GAA GAC TGG ATA ACTGTC3′and reverse primer 5′ AGT CGA CAG GAT GCA GAG GCT G 3′. The oligonucleotide primers for β actin were forward primer 5′ GGCACCACCTTCTACAATG3′ and reverse primer 5′GGGGTGTTGAAGGTCAAAC 3′. P53 gene expression levels in hepatic tissues were analyzed by using quantitative real-time PCR (qRT-PCR) by using real time PCR machine (3000x Agilent Technologies, Santa Clara, CA, USA). The cycle of threshold (Ct) value was determined, and the abundance of gene transcripts were analyzed by using the ΔΔCt method using β-actin as a housekeeping gene for correction of the expression.[35] The expression in the hepatic tissue of the control mice was set to one.

Immunohistochemistry for Detection of Caspase-3 Protein in Hepatic Tissue

The serial sections of hepatic tissue were dewaxed and dehydrated sequentially in graded ethyl alcohol. Then they were immersed in antigen retrieval solution (EDTA solution, pH 8). The endogenous peroxidase was inactivated by 3% H_2O_2 and the reaction was blocked by 5% BSA blocking reagent for 20 min to reduce nonspecific reactions. Then, the fixed sections were incubated with anticaspase-3 primary monoclonal antibody (R&D Systems Inc., Minneapolis, MN, USA; 1:100 dilutions) for one hour at 37°C. The slides were rinsed with PBS, incubated with antimouse IgG secondary antibodies (EnVision+System HRP; Dako, Denmark A/S, Glostrup, Denmark) for 30 min at room temperature, visualized with diaminobenzidine commercial kits (Liquid DAB+Substrate Chromogen System; Dako), and finally counterstained with Mayer's hematoxylin. The normal mouse serum was used instead of primary antibody to stain the negative control. The caspase-3 protein expression was expressed as the percentage of positive cells per total 1000 cells in about eight to 10 microscopic fields.

Histopathological Examination

The fixed specimens of liver, kidneys and spleen were processed, embedded in paraffin, cut and stained by H&E stain. Stained slides were microscopically analyzed by using a light microscope. Histopathological photos were taken by using a digital Leica photomicroscope (Leica, Microsystems, Wetzlar, Germany).

Statistical Analysis

Data were presented as mean ±SEM. Data were analyzed by one-way ANOVA followed by Duncan's post hoc analysis for detection of significance among different groups. The statistical analysis was performed by using SPSS (Statistical Package for Social Sciences) Version 16 released in 2007 (SPSS Inc., Chicago, IL, USA) for data analysis to determine the statistically significant ($P<0.05$) differences among the experimental groups.

Results

Morphological and Structural Characters of Synthesized Copper Nanoparticles

Analysis by TEM

Figure 1 showed the micrograph obtained from TEM of the biologically and chemically synthesized CuO-NPs. The biologically synthesized NPs were predominantly spherical in shape (Figure 1A) whereas chemically synthesized NPs ranged from spherical to elongated shape (Figure 1B). The size of biologically synthesized CuO-NPs ranged from 13.97–21.22 nm (Figure 1A) while that of chemically synthesized CuO-NPs ranged from 20.61–29.51 nm (Figure 1B).

Analysis by XRD

The size of biologically synthesized CuO-NPs ranged from (4.14 to 12.82 nm) and that of chemically synthesized ones ranged from (4.06 to 26.82 nm) (Tables 1 and 2).

Furthermore, the results of Figure 1 investigated the peak positions with 2Θ (Zeta) values of 16.36, 22.62, 27.77, 31.74, 35.43, 41.14, 52.37, 56.07, 60.02, 66.55 and 73.64, which were indexed as 100, 110, 111, 200, 210, 211, 221, 310, 311, 222 and 320 for biologically synthesized CuO-NPs (Figure 1C) and the peak positions with 2Θ values of 36.17, 42.10, 43.03, 50.11, 61.09 and 73.83 were indexed as 111, 200, 210, 211, 220 and 221 for chemically synthesized CuO-NPs (Figure 1D). These results confirmed that the obtained particles of CuO-NPs are crystalline.

Analysis by FT-IR

In this study, FT-IR spectroscopy data illustrated in Figure 1E and F and Table 3 indicated that band

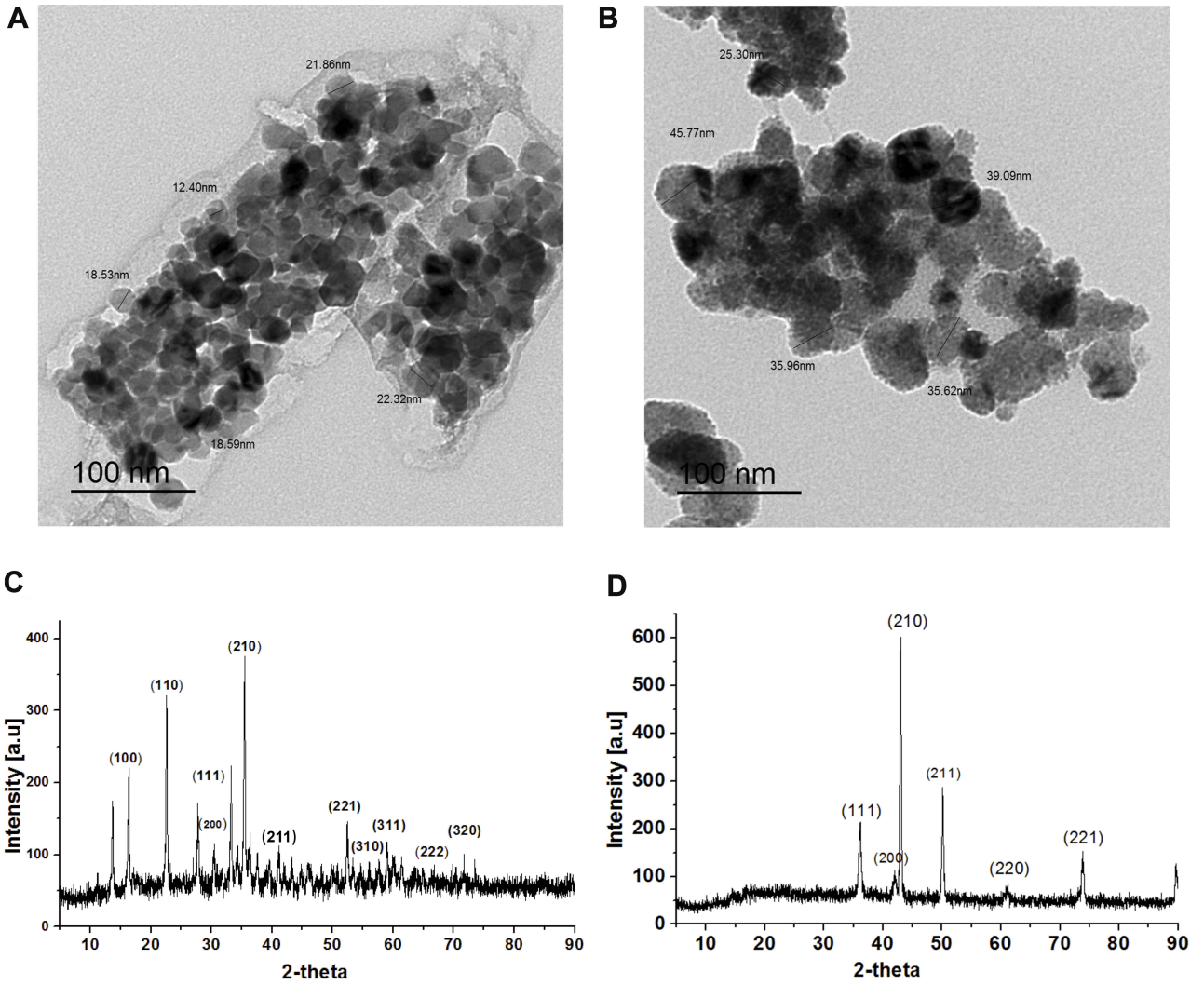

Figure 1 Continued.

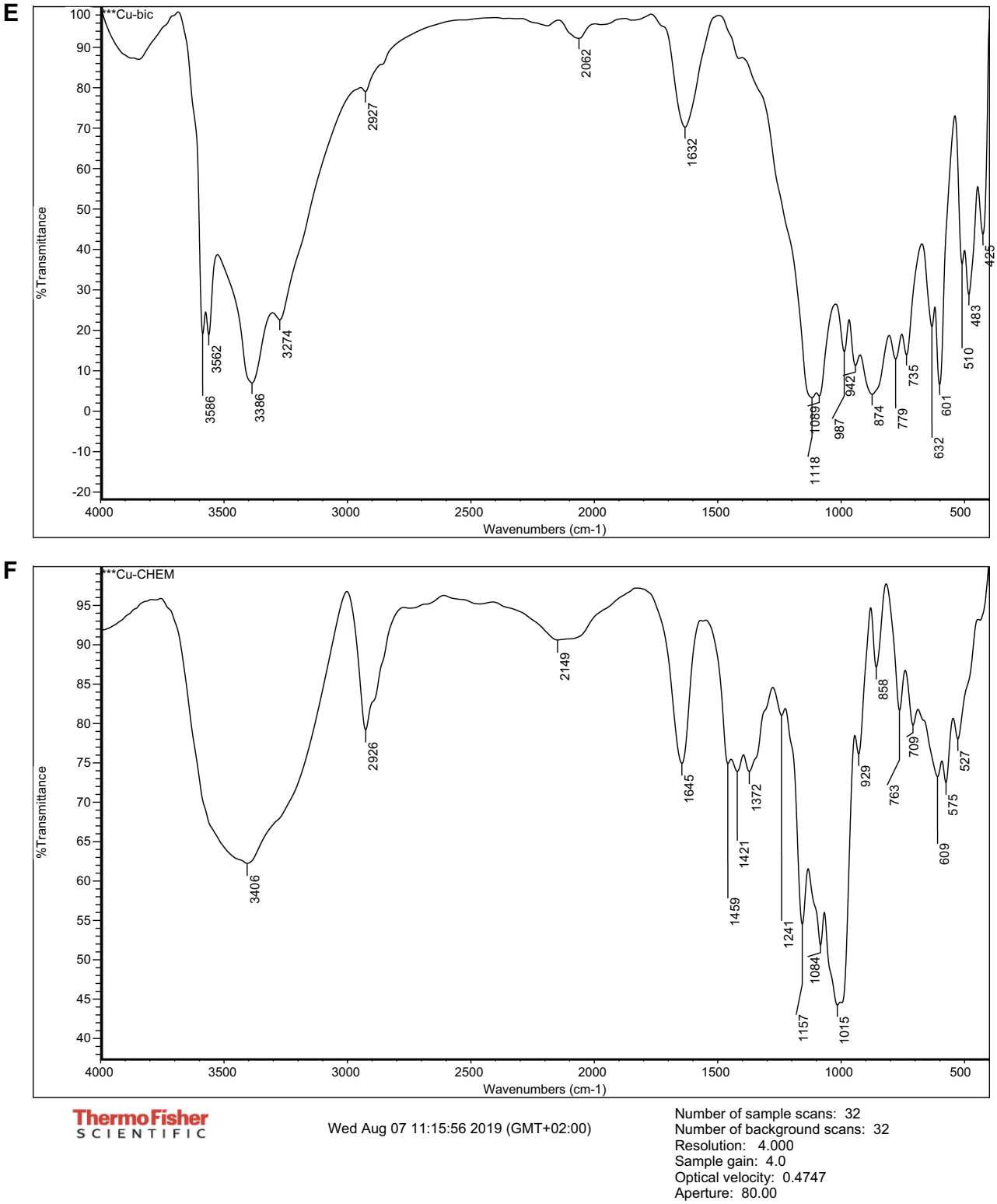

Figure 1 Morphological and structural patterns of biologically synthesized (**A**) and chemically synthesized (**B**) CuO-NPs by TEM; XRD of biologically synthesized (**C**) and chemically synthesized (**D**) CuO-NPs; FT-IR spectrum of biologically synthesized (**E**) and chemically synthesized (**F**) CuO-NPs.

Table 1 The Particle Size by XRD of Biologically Synthesized CuO-NPs

Pos. (°2θ)	FWHM Left (°2θ)	Diameter (nm) Particle Size	Rel. Int. (%)
16.3670	0.1968	7.34	50.34
22.6259	0.1771	8.48	92.12
31.7454	0.3936	4.14	6.63
35.4300	0.1574	10.81	100.00
41.1439	0.1968	9.35	15.39
52.3742	0.1771	12.82	27.12
56.0784	0.4723	5.25	6.01
60.0289	0.3936	7.05	12.45
66.5577	0.7872	4.42	2.75
73.6423	0.4723	10.41	5.13

Abbreviation: FWHM, full width at half maximum.

Table 2 The Particle Size by XRD of Chemically Synthesized CuO-NPs

Pos. (°2θ)	FWHM Left (°2θ)	Diameter (nm) Particle Size	Rel. Int. (%)
36.1758	0.2755	4.06	26.63
42.1079	0.4330	4.31	7.76
43.0339	0.1771	26.829	100.00
50.1117	0.2755	7.84	41.88
61.0938	0.6298	4.55	4.78
73.8376	0.2952	16.87	16.97

Abbreviation: FWHM, full width at half maximum.

regions 3586, 3562, 3386 and 3274 cm^{-1} for CuO-NPs synthesized by the biological method and regions 3406 and 1645 cm^{-1} for CuO-NPs synthesized by the chemical method related to OH groups. The peak in the region 2927 cm^{-1} for biogenic CuO-NPs and 2926, 1459, 1421 and 1372 cm^{-1} for chemical CuO-NPs regions originated from C–H (hydrocarbon). The peaks in the region 2062 and 874 cm^{-1} for biologically synthesized CuO-NPs and 2149 and 929 cm^{-1} for chemically synthesized CuO-NPs can be correlated to stretching of Cu–H (metal–hydrogen) and Cu-O-H respectively. The bands in the 1632 cm^{-1} that appear in biogenic method could be related to amides (N-H) stretching. In addition four band regions of C–O in both CuO-NPs were detected. The peaks appeared in the range from 779 cm^{-1} to 425 cm^{-1} for biologically synthesized CuO-NPs and from 858 cm^{-1} to 524 cm^{-1} for chemically synthesized CuO-NPs were the Cu-O group indicating the formation of CuO-NPs at many peaks.

Table 3 Fourier-Transform Infrared Analysis of Biologically Synthesized and Chemically Synthesized CuO-NPs

Biologically Synthesized CuONPs		Chemically Synthesized CuONPs	
Wave Numbers cm^{-1}	Functional Groups	Wave Numbers cm^{-1}	Functional Groups
3586	O–H stretching	3406	O–H stretching
3562	O–H stretching	2926	C–H stretching
3386	O–H stretching	2149	Cu–H stretching
3274	O–H stretching	1645	O–H bending
2927	C–H stretching	1459	C–H bending
2062	Cu–H stretching	1421	C–H bending
1632	N-H stretching	1372	C–H bending
1118	C–O stretching	1241	C–O stretching
1089	C–O stretching	1157	C–O stretching
987	C–O stretching	1084	C–O stretching
942	C–O stretching	1015	C–O stretching
874	Cu–O–H bending	929	Cu–O–H bending
779	Cu–O	858	Cu–O–H bending
735	Cu–O	763	Cu–O
632	Cu–O	709	Cu–O
601	Cu–O	609	Cu–O
510	Cu–O	575	Cu–O
483	Cu–O	524	Cu–O
425	Cu–O		

Clinical Signs and Necropsy Findings of Animals Intoxicated with CuO-NPs

The main signs of CuO-NPs intoxication were loss of appetite, depression and lowering of activity.

Four mice died from the group that received biologically synthesized CuO-NPs. The necropsy finding revealed that stomachs of biologically synthesized CuO-NPs administered mice were distended with greenish colored ingesta while stomachs of chemically synthesized CuO-NPs administered mice were distended with brownish colored ingesta. Enlarged liver, gunmetal colored kidney, dark swollen spleen and distended urinary bladder were observed in both CuO-NPs oral gavaged mice. Urinary bladders of biologically synthesized CuO-NPs oral gavaged mice were filled with reddish yellow urine.

Copper Oxide Nanoparticles Intoxication Altered Total and Differential Leucocyte Counts in Mice

The effects of Copper oxide nanoparticles on hematological parameters of mice were recorded in Table 4.

Table 4 Mean Values of RBC Count, HGB Concentration, HCT%, Leukocyte Count and Differential Leukocyte Percentages of Control and CuO-NPs Administered Mice

	RBCs $\times 10^6$/µL	HGB (g/dl)	HCT%	TLC $\times 10^3$/µL	Lymphocytes %	Monocytes %	Granulocytes %
Control	7.45 ± 0.28^{a}	11.34 ± 0.25^{a}	30.58 ± 0.66^{ab}	3.8 ± 0.27^{b}	32.18 ± 0.63^{b}	20.38 ± 0.24^{a}	47.44 ± 1.08^{b}
Biologically CuO-NPs	6.84 ± 0.37^{a}	10.62 ± 0.49^{a}	28.58 ± 0.67^{b}	4.3 ± 0.26^{ab}	36.74 ± 0.69^{a}	21.26 ± 0.88^{a}	42.00 ± 1.30^{c}
Chemically CuO-NPs	7.73 ± 0.14^{a}	11.42 ± 0.22^{a}	32.16 ± 0.75^{a}	4.7 ± 0.24^{a}	26.06 ± 0.84^{c}	22.46 ± 0.65^{a}	51.48 ± 0.92^{a}

Notes: Data are presented as means ± SEM (n=10). Values having different superscript letters within same column are significantly different ($P<0.05$).
Abbreviations: RBCs, red blood cells; HGB, hemoglobin; HCT, hematocrit; TLC, total leukocytes count.

Biologically synthesized CuO-NPs numerically reduced the RBC count; HGB concentration and HCT% compared with those of the control and chemically synthesized CuO-NPs mice. However, biologically synthesized CuO-NPs numerically elevated the total leucocyte counts and significantly increased lymphocyte percentages while it significantly decreased the granulocyte percentage at $P<0.05$ compared with the control mice. Chemically synthesized CuO-NPs significantly elevated total leukocyte count and granulocyte percentage but significantly reduced lymphocyte percentage (lymphocytopenia) compared with those of the control mice ($P<0.05$).

Copper Oxide Nanoparticles Altered Hepatic and Renal Functions in Mice

Figure 2 represented the effects of both biologically and chemically synthesized CuO-NPs on serum hepatic and renal function biomarkers of mice. Oral administration of mice with biologically synthesized and chemically synthesized CuO-NPs significantly elevated the activities of serum ALT and AST compared with those of the control group at $P<0.05$. In addition, they significantly increased serum levels of renal biomarkers, serum urea and creatinine, compared with those of the control mice. Moreover, mice administered biologically synthesized CuO-NPs showed significant increase in serum urea and creatinine levels compared to mice administered with chemically synthesized CuO-NPs.

Biologically Synthesized Copper Oxide Nanoparticles Increased P53 mRNA Expression in Hepatic Tissues of Mice

Administration of mice biologically synthesized CuO-NPs dramatically elevated the relative mRNA expression of P53 (1042.42±693.18) at P<0.05 compared to those of the normal control (1±0.14) and chemically synthesized CuO-NPs (1.04±0.09) administered mice. In contrast, chemically synthesized CuO-NPs administration had no significant effect on the relative mRNA expression of P53 in hepatic tissues compared to that of the normal control mice.

Copper Oxide Nanoparticles Intoxication Increased Caspase-3 Protein Expression in Hepatic Tissues of Mice

Figure 3 illustrated the microscopic pictures of immunohistochemistry and mean values of positively stained hepatocytes (in percent) for caspase-3, proapoptotic biomarker, in hepatic tissues. Hepatic tissues of normal control mice showed negative or mild caspase-3 immunostaining (Figure 3A1 and A2), respectively. Hepatocytes of biologically synthesized CuO-NPs administered mice showed marked caspase-3 immunostaining especially around the central vein (Figure 3B1 and B2) and significantly elevated the percent of caspase-3 immunostained hepatocytes to 60.79 ±1.79 compared to that of the normal control mice 9±0.45 (Figure 3D). Hepatocytes of chemically synthesized CuO-NPs administered mice showed a moderate degree of caspase-3 immunostained hepatocytes (Figure 3C1 and C2) and also significantly elevated the percent of caspase-3 immunostained hepatocytes to 21.23±0.89 compared to that of the normal control mice 9±0.45 (Figure 3D).

Copper Oxide Nanoparticles Altered Hepatic, Renal and Splenic Tissues Architectures in Mice

Histopathological changes in hepatic, renal and splenic tissues due to intoxication of rats with CuO-NPs were illustrated in Figures 4–6.

Microscopical examination of hepatic tissues of control mice showed normal architecture of hepatic tissue (Figure 4A). Mice that received biologically synthesized CuO-NPs showed various pathological alterations in hepatic tissue such as activation of Kupffer cells, lymphocytic infiltration around necrotized cells, congestion and

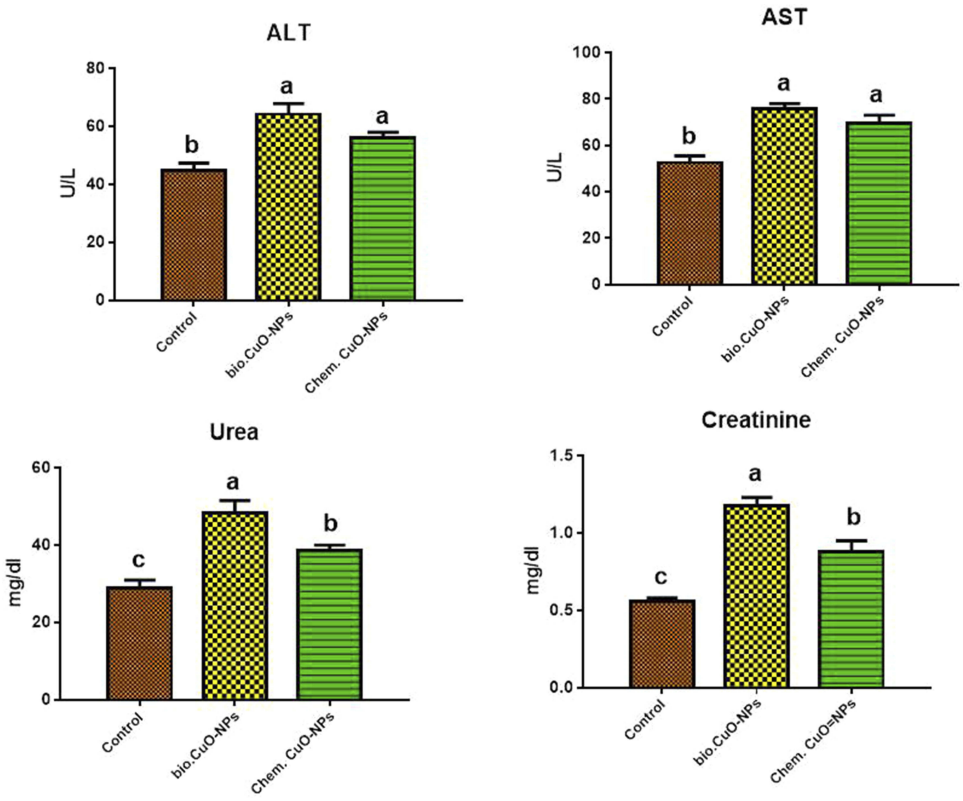

Figure 2 Mice received distilled water (control), a single dose of biologically synthesized CuO-NPs (500 mg/kg bw) (second group) or a single dose of chemically synthesized CuO-NPs (500 mg/kg bw) orally (third group). The activities of serum ALT, AST and serum levels of urea and creatinine of the control and CuO-NPs treated mice were determined. Columns with different letters were significantly different ($P< 0.05$).

hepatocytes pathological changes. These changes ranged from hydropic degeneration and vacuolization to cell necrosis, loss of cellular boundaries, more eosinophilic cytoplasm, karyorrhexis and some cells lost their nucleus (Figure 4B1 and B2). Hepatic tissues of mice administered with chemically synthesized CuO-NPs showed only hydropic degeneration, activation of Kupffer cells and slight degree of fatty changes (Figure 4C1 and C2).

Figure 5 showed histopathological changes in renal tissues of normal and CuO-NPs administered mice. Renal tissue of control mice showed normal renal tubules and glomeruli (Figure 5A). Renal tissues of biologically synthesized CuO-NPs administered mice showed glomerular hypercellularity, severe coagulative necrosis, detached tubular epithelia, loss of brush border and intraluminal hyaline casts in cortex and medulla (Figure 5B1 and B2). Renal tissues of chemically synthesized CuO-NPs administered mice showed intertubular hemorrhage, cloudy swelling, narrowing of tubular lumen, glomerular hypercellularity, pyknotic nuclei and tubular cell necrosis (Figure 5C1 and C2).

Figure 6 presented histopathological changes in splenic tissues of normal and CuO-NPs administered mice. Spleen tissue of control mice was normal histological structure (Figure 6A). This figure showed presence of many pathological lesions and deviation in splenic tissues of CuO-NPs administered mice compared with those of normal control mice. Biologically synthesized CuO-NPs led to lymphoid depletion with presence of large number of megakaryocytes and hemosiderin phagocytic cells (hemosidrophages) in splenic tissue (Figure 6B1 and B2). Chemically synthesized CuO-NPs induced the same changes but with a lower degree of lymphoid depletion with presence of fewer numbers of megakaryocytes in splenic tissue (Figure 6C1 and C2).

Discussion

Nanocopper has been used as a novel antibacterial agent for treatment of osteoporosis, for manufacturing of intrauterine contraceptive device, and feed additives for cattle and poultry.[9] When ionized copper intake exceeds the tolerable limit, it shows toxic effects leading to

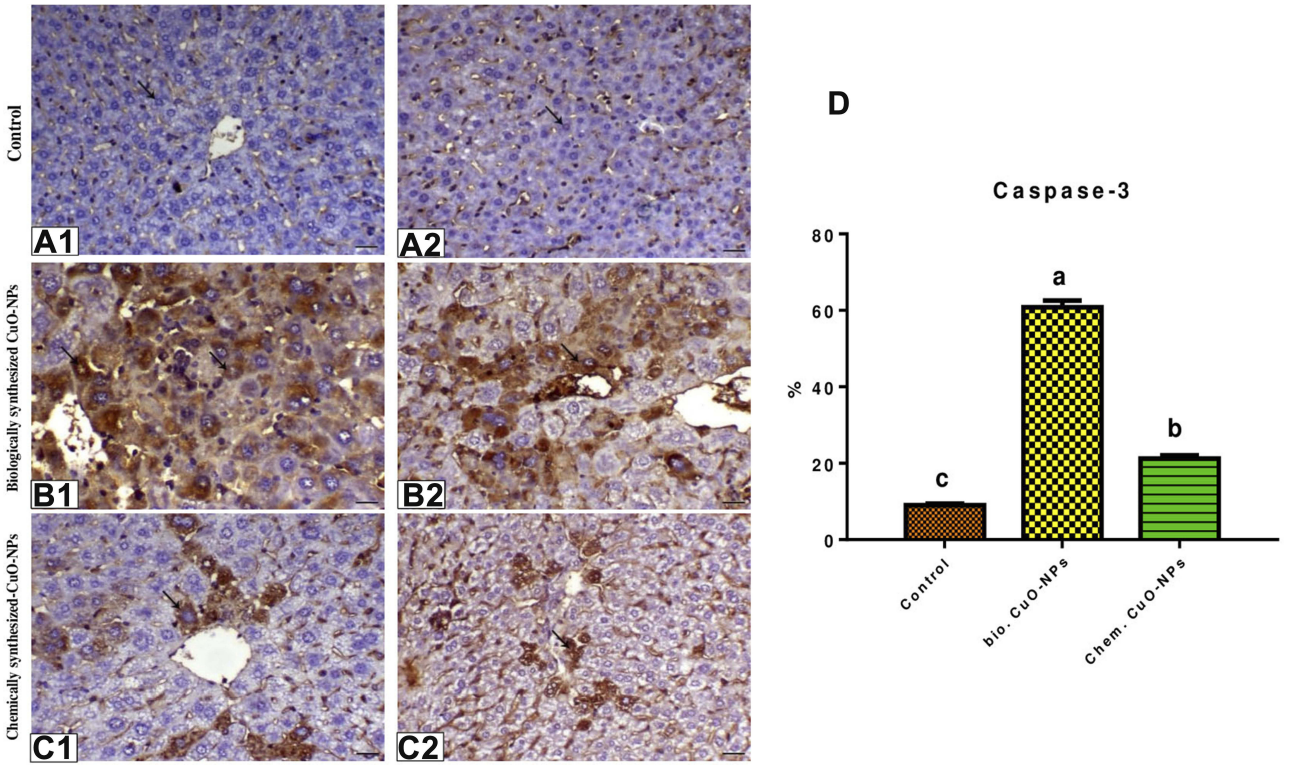

Figure 3 Photomicrographs of liver sections showed immunoreactivity to caspase-3. (**A1**) Liver of control animal showing negative expression of caspase antibody (arrow), caspase-3 IHC, bar=40 µm. (**A2**) Liver of control animal showing mild caspase immunostaining (arrow), caspase-3 IHC, bar=40 µm. (**B1**) Liver of biologically synthesized CuO-NPs treated mice showing marked centrolobular immunostaining of caspase (arrow), caspase-3 IHC, of G2 animal bar=40 µm. (**B2**) Liver of biologically synthesized CuO-NPs animal showing marked centrolobular immunostaining of caspase (arrow), caspase-3 IHC, bar=40 µm. (**C1**) Liver of chemically synthesized CuO-NPs treated mice showing moderate degree of centrolobular immunostaining of caspase (arrow), caspase-3 IHC, bar=40 µm. (**C2**) Liver of chemically synthesized CuO-NPs treated mice showing moderate degree of centrolobular immunostaining of caspase (arrow), caspase-3 IHC, bar=40 µm. (**D**) Caspase-3 protein expression was expressed as the percentage of positive cells per total 1000 cells. Columns with different superscript letters were significantly different ($P<0.05$).

cytotoxicity and cell death.[36] In the current study, green (biologically) and chemically synthesized CuO-NPs were characterized by TEM, XRD, and FT-IR to determine their sizes and functional groups. These tests revealed that the NPs are mainly in the form of CuO-NPs and the biologically synthesized (spherical particles) CuO-NPs are smaller in size than chemically synthesized CuO-NPs (elongated or spherical particles) and so recorded wide size range. Different functional groups (O-H, C-H, C-O, Cu-H and CuO) were detected by FT-IR. In this study, TEM and XRD results were inconsistent with those of Abboud et al,[27] who indicated that the maximum size of CuO particles ranged from 5 to 45 nm, and the average size was estimated as 20.66 nm. Also Siddiqi and Husen[37] reviewed that the TEM image of the majority of CuO-NPs are spherical, but some of them are elongated. It has been reported that the size and the shape of NPs differ according to the method and factor affecting their synthesis.[38,39]

Fourier-transform infrared spectroscopy was used to detect the stretching and bending frequencies of molecular functional groups that attached to the surface of CuO-NPs causing structural and conformational changes.[40,41] The absorption position of infrared bands depends on the force constant of a chemical bond, bond order, types of atoms joined by the bond, and reduced mass. The peak intensity in the infrared spectra is determined by the concentration of molecules in the sample.[42,43] The bands in the 1632 cm^{-1} that appear in biogenic methods could be related to amides (N-H) stretching, which may help in stabilizing the NPs by proteins.[44] The small peak shift in the vibrational modes is associated with the corresponding change in the surface area of the prepared CuO-NPs.[45] In addition, Yedurkar et al[46] recorded three absorption peaks that revealed the vibrational modes of CuO nanostructures in the range 700–400 cm^{-1} and these foremost peaks were detected as 525, 580, and 675 cm^{-1}.

The results of this study revealed that the administration of the biologically synthesized CuO-NPs to mice induced numerical reduction in RBC count, HGB concentration and

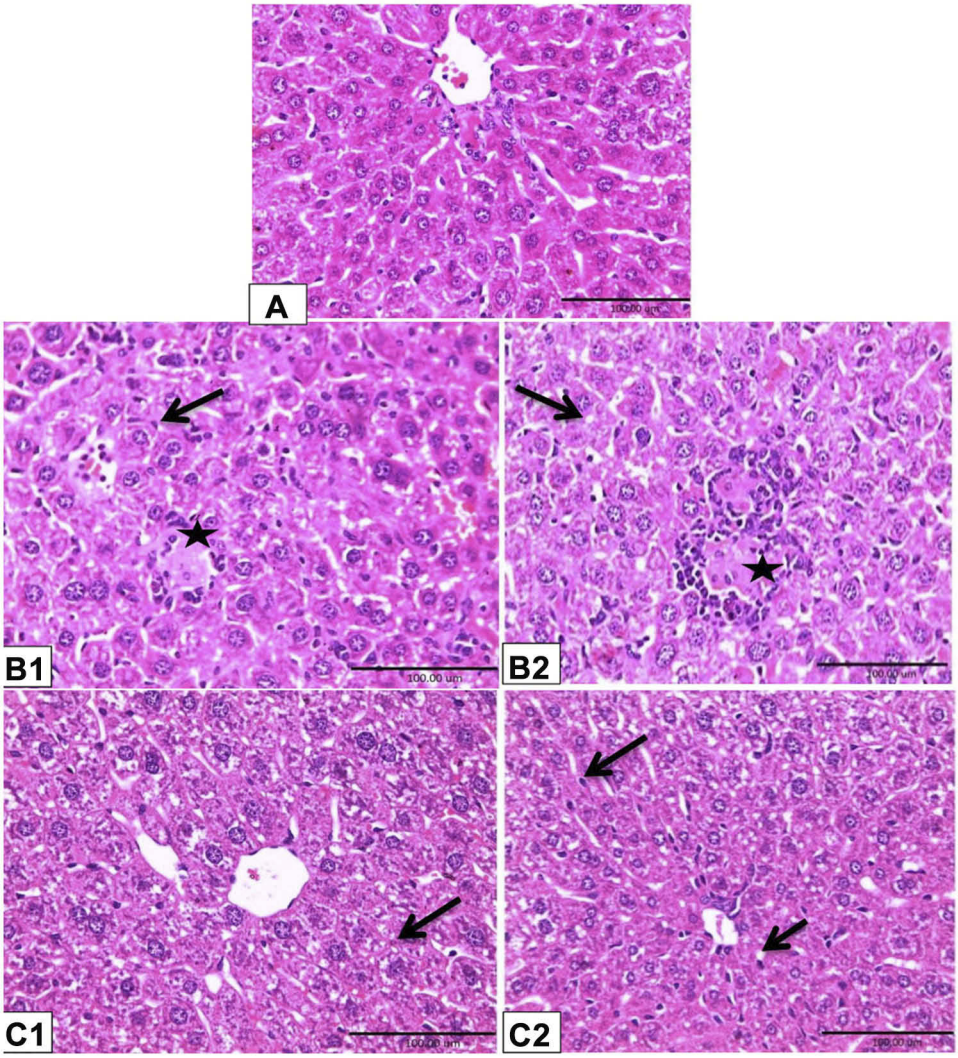

Figure 4 Photomicrographs of mice liver tissues. Rats were treated as Figure 2. Hepatic tissues of control mice (**A**) showed normal tissue architecture. Hepatic tissues of biologically synthesized CuO-NPs exposed mice showed activation of Kupffer cells (arrow), hepatocytes necrosis and loss of cellular boundaries (star) (**B1**); hydropic degeneration of hepatocytes (arrow), lymphocytic infiltration around necrotized cells (star) (**B2**). Hepatic tissues of chemically synthesized CuO-NPs exposed mice showed hydropic degeneration (arrow) (**C1**) and slight degree of fatty change (short arrow) and activation of Kupffer cells (long arrow) (**C2**) (H&E ×40).

HCT%, while chemically synthesized CuO-NPs slightly elevated these parameters compared to those of the control mice (Table 4). These findings can be explained by the incidence of the acute hemolysis in mice administered with biologically synthesized CuO-NPs, indicated by the presence of red urine in the urinary bladder at necropsy, presence of hyaline and granular casts in renal tubules (Figure 5), and hemosiderophages in splenic tissue (Figure 6). In addition, biologically synthesized CuO-NPs led to deaths among mice, which may refer to severe hepatic necrosis (Figure 4), RBC damage and presence of red urine within two days of exposure, these findings were parallel with the findings reported by Ortolani et al.[47] The possible reason for RBC destruction and hemolysis is the inhibition of glucose-6-phosphate dehydrogenase induced by acute copper poisoning leading to the reduction of NADPH concentration in the red blood cells and subsequently decreased the level of reduced glutathione, and hence the occurrence of hemolysis.[48] Moreover, the sudden increase in blood copper concentration in acute toxicity leads to methemoglobinemia, formation of Heinz bodies and ROS induced lipid peroxidation of erythrocyte membranes resulting in intravascular hemolysis of damaged erythrocytes.[49,50] In contrast, both biologically and chemically synthesized CuO-NPs increased total leukocyte count as a result of lymphocytosis in biologically synthesized CuO-NPs and granulocytosis in chemically synthesized CuO-NPs (Table 4). These findings were matched with those of Bugata et al[15] who reported that

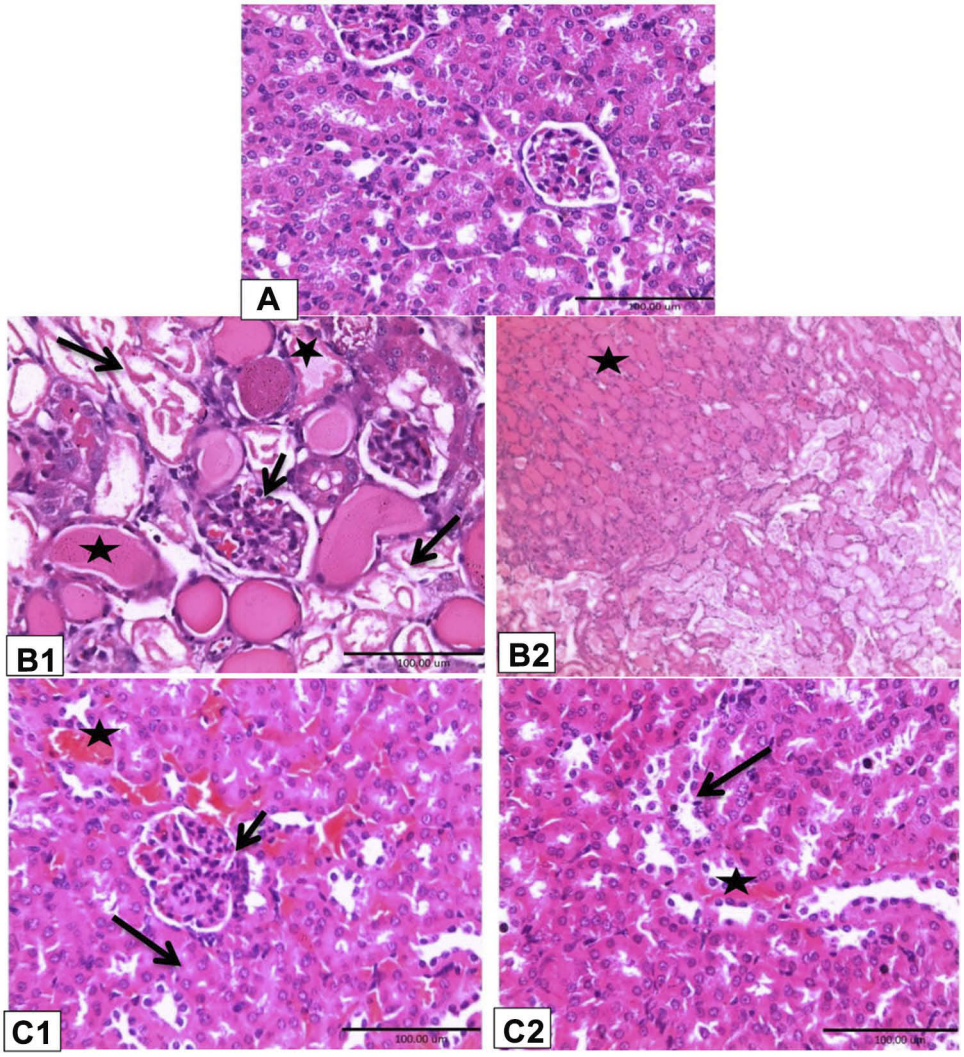

Figure 5 Photomicrographs of mice renal tissues. Rats were treated as Figure 2. Renal tissues of control mice showed normal renal tubules and glomeruli (**A**) (H&E ×40). Renal tissues of biologically synthesized CuO-NPs exposed mice showed glomerular hypercellularity (short arrow); severe coagulative necrosis, detached tubular epithelia and loss of brush border (long arrow); intraluminal hyaline casts (black star) in cortex (**B1**) (H&E ×40) and medulla (black star) (**B2**) (H&E ×10). (**C1, C2**) Chemically synthesized CuO-NPs exposed mice showed intertubular hemorrhage (star); cloudy swelling with, narrowing of tubular lumens (long arrow); glomerular hypercellularity (short arrow) (**C1**); pyknotic nuclei and tubular cell necrosis (long arrow) and intertubular hemorrhage (star) (**C2**) (H&E ×40).

CuO-NPs at 2000 mg/kg bw increase RBC and WBC counts and hemoglobin concentration in rats. Moreover, exposure of fish to copper for 96 h induces leukocytosis, lymphocytosis and neutropenia.[51] This increase in the WBC count may indicate the intrinsic protection and initiation of the body's defense mechanism.[52]

Furthermore, this study indicated that administration of mice with CuO-NPs disturbed liver and kidney functions and structures indicated by increased activities of serum ALT and AST and serum levels of both urea and creatinine and appearance of various pathological alterations in the structure of liver, kidney, and spleen. These alterations were more prominent in mice administered with biologically synthesized CuO-NPs. These findings were in accordance with those reported by[15,31,53] in rats and mice after exposure to a single acute dose of Cu-NPs or CuO-NPs. In addition, it has been indicated that green synthesized gold–copper selenium heterogeneous nanoparticles induce in vitro cytotoxicity[54] as copper nanoparticles have been reported to generate ROS and reactive nitrogen species (RNS), which play an important role in induction of organ injuries and dysfunctions.[55] The toxic effects of CuO-NPs in the present study might be related to the induction of oxidative stress, which subsequently increased protein expression of caspase-3 in hepatic tissue (Figure 3) as the exposure to CuO-NPs increases ROS production that activates signal transduction of mitochondrial membrane and releases of cytochrome c from the

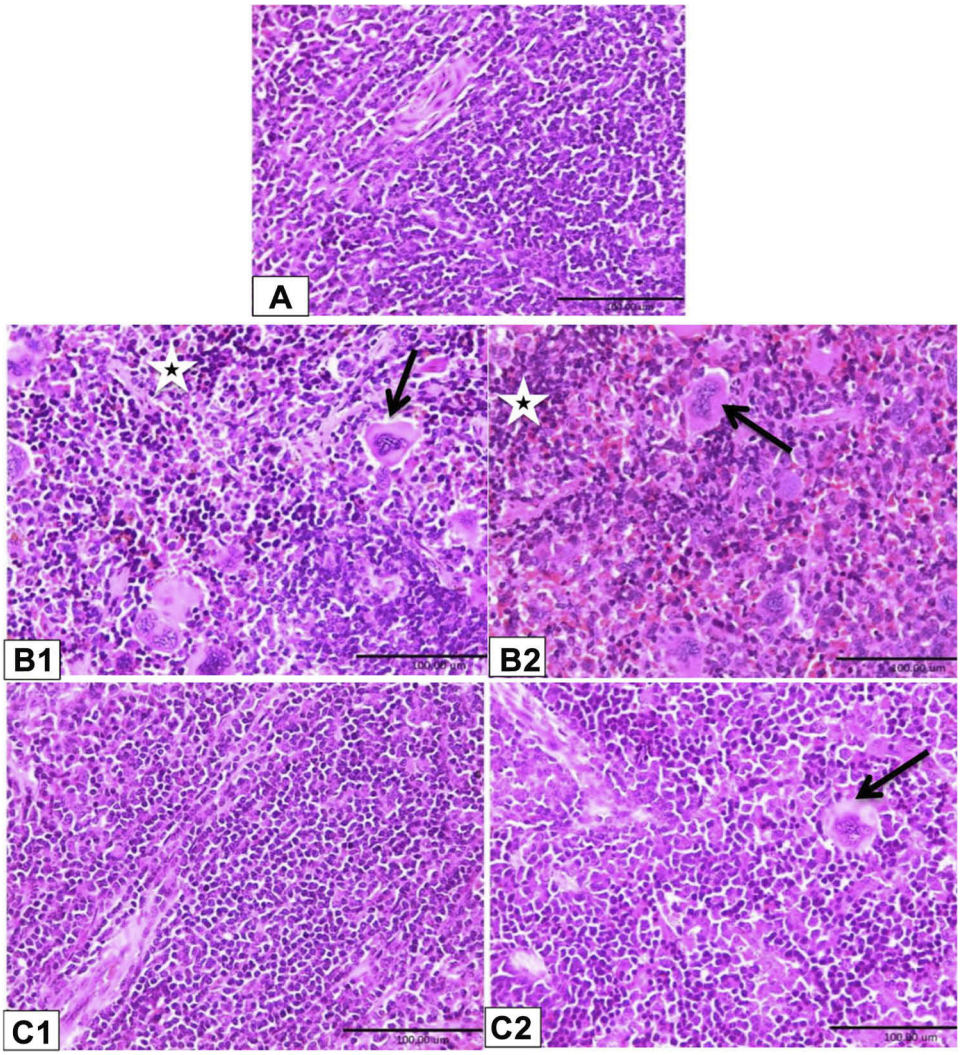

Figure 6 Photomicrographs of mice splenic tissues. Rats were treated as Figure 2. Spleen tissues of control mice (**A**) showed normal histological structure. Spleen tissues of biologically synthesized CuO-NPs exposed mice showed lymphoid depletion, presence of large number of megakaryocytes (arrow) and hemosiderophages (star) (**B1** and **B2**). Spleen tissues of chemically synthesized CuO-NPs exposed mice showed moderate degree of lymphoid depletion and presence of few numbers of megakaryocytes (arrow) (**C1** and **C2**) (H&E ×40).

mitochondria to the cytosol. Release of cytochrome c to the cytosol in turn activates caspase-9, a cysteine protease that can activate caspases-3 and 7, which are responsible for destroying the cell.[56–58] Thus, CuO-NPs can trigger both intrinsic and extrinsic apoptotic pathways in response to oxidative stress.[54] Furthermore, administration of mice with either biologically or chemically synthesized CuO-NPs increased gene expression of P53 and protein expression of caspase-3 in hepatic tissues because apoptosis or self-destruction is activated under the action of P53 when DNA damage occurred and this damage cannot be resolved by the repair system.[59]

Histopathological investigations of liver, kidney, and spleen in the present study illustrated presence of several alterations in these organs accompanied with hepatic and renal dysfunction. These lesions were more prominent in biologically synthesized CuO-NPs (Figures 4–6). Similarly, pathological alteration was demonstrated[53,60] in hepatic, renal, and splenic tissues of mice after acute exposure to a high dose of Cu-NPs and in liver and kidneys of rats exposed to single high dose of CuO-NPs.[15] These detrimental effects of CuO-NPs occurred due to the nanoparticles can be absorbed across the gastrointestinal tract, and pass through the mesentery lymph supply and lymph node to liver and spleen; where reticuloendothelial system can accumulate copper from blood by phagocytosis, predominantly NPs, which have not been completely dissolved.[61,62] The accumulated NPs led to

lymphocytic infiltration and increased the number of Kupffer cells in the liver and megakaryocytosis with lymphoid depletion in spleen tissue. It has been indicated that Cu-NPs are observed in the vascular areas of the periportal hepatocytes and in the cytoplasm of the Kupffer cells of the liver in treated rats.[55] Various pathological changes observed in renal tissues in mice administered with biologically synthesized CuO-NPs may be due to hemoglobinuria caused by intravascular hemolysis and direct action of copper on the kidneys leading to tubular necrosis and acute renal failure.[63] In addition, kidneys accumulate mostly the copper in ionic form after the dissolution of NPs in vivo.[62] Copper ion overload in the kidneys may occur after high absorption and rapid distribution of biologically synthesized CuO-NPs due to their smaller size and exceeding copper binding protein capacities. Previously it has been proven that high reactivity of nanocopper particles caused wide toxicological difference between small size (23.5 nm) and big size (17 µm) particles, the copper ion overload in small size particles is consistent with biochemical assay, pathological lesions and copper content in renal tissue.[61] Therefore, there are two possible mechanisms through which CuO-NPs induced alterations in liver, kidney, and spleen functions and structures. (1) CuO-NPs induced oxidative stress that increases the production of proapoptotic cytokine, caspase-3, which subsequently induced tissue injuries. (2) The accumulation of CuO-NPs in tissues which disturbed their function and structures.

The uptake and distribution of NPs depends on their size and surface area.[64] The results of the current study revealed that biologically synthesized CuO-NPs have more potent toxic effects than chemically synthesized CuO-NPs. This might be attributed to the size of NPs as the biologically synthesized CuO-NPs had smaller, spherical shaped particles while chemically synthesized CuO-NPs had a larger size range and spherical or elongated particles. Previous studies[61,65] demonstrated that the in vivo toxic effects of nanocopper particles were more prominent than microcopper particles depending on mass basis, huge specific surface area and high solubility in physiological milieus of Cu-NPs when administered orally. Mortimer et al[66] quantifed the size-dependent toxic impact of CuO-NPs and indicated that they were 10 to 20 times more toxic than its bulk form.

Conclusion

This study indicated that administration of a high dose of biologically and chemically synthesized CuO-NPs induced hematological, biochemical, apoptotic and pathological changes. The biologically synthesized CuO-NPs induced more vigorous degrees of tissue damage than chemically synthesized CuO-NPs referring to the differences in the size and shape of the synthesized NPs and content of functional groups.

Acknowledgment

The authors are grateful to the Deanship of Scientific Research, King Saud University, for funding through Vice Deanship of Scientific Research Chairs.

Disclosure

The authors report no conflicts of interest in this work.

References

1. Yah CS, Simate GS, Iyuke SE. NPs toxicity and their routes of exposures. *Pak J Pharm Sci*. 2012;25(2):477–491.
2. Society of Toxicology. Developing safe products using nanotechnology. Avialable from: http://www.toxicology.org. (accessed 20 April, 2012).
3. Shanmuganathan R, LewisOscar F, Shanmugam S, et al. Core/shell nanoparticles: synthesis, investigation of antimicrobial potential and photocatalytic degradation of Rhodamine B. *J Photochem Photobiol B*. 2020;202:111729. doi:10.1016/j.jphotobiol.2019.111729
4. Prabhu R, Rajmohamed MA, Anjali R, et al. Ecofriendly one pot fabrication of methyl gallate@ZIF-L nanoscale hybrid as pH responsive drug delivery system for lung cancer therapy. *Process Biochem*. 2019;84:39–52. doi:10.1016/j.procbio.2019.06.015
5. Bhattacharya S, Alkharfy KM, Janardhanan R, et al. Nanomedicine: pharmacological perspectives. *Nanotechnol Rev*. 2012;1(3):235–253. doi:10.1515/ntrev-2011-0010
6. Oberdorster G. Safety assessment for nanotechnology and nanomedicine: concepts of nanotoxicology. *J Intern Med*. 2010;267(1):89–105. doi:10.1111/j.1365-2796.2009.02187.x
7. Aillon KL, Xie Y, El-Gendy N, et al. Effects of nanomaterials physicochemical properties on in vivo toxicity. *Adv Drug Deliv Rev*. 2009;61(6):457–466. doi:10.1016/j.addr.2009.03.010
8. Kang M, Lim CH, Han JH. Comparison of toxicity and deposition of nano-sized carbon black aerosol prepared with or without dispersing sonication. *Toxicol Res*. 2013;29(2):121–127. doi:10.5487/TR.2013.29.2.121
9. Liu G, Li X, Qin B, et al. Investigation of the mending effect and mechanism of copper nanoparticles on a tribologically stressed surface. *Tribol Lett*. 2004;17(4):961–966. doi:10.1007/s11249-004-8109-6
10. Ebrahimnia-Bajestan E, Niazmand H, Duangthongsuk W, et al. Numerical investigation of effective parameters in convective heat transfer of nanofluids flowing under a laminar flow regime. *Int J Heat Mass Transf*. 2011;54(19–20):4376–4388. doi:10.1016/j.ijheatmasstransfer.2011.05.006
11. Chirieac A, Dragoi B, Ungureanu A, et al. Facile synthesis of highly dispersed and thermally stable copper-based nanoparticles supported on SBA-15 occluded with P123 surfactant for catalytic applications. *J Catal*. 2016;339:270–283. doi:10.1016/j.jcat.2016.04.004
12. Esteban-Tejeda L, Malpartida F, Esteban-Cubillo A, et al. Antibacterial and antifungal activity of a soda-lime glass containing copper nanoparticles. *Nanotechnology*. 2009;20(50):50570.

13. Ingle AP, Duran N, Rai M. Bioactivity, mechanism of action, and cytotoxicity of copper-based nanoparticles: a review. *Appl Microbiol Biotechnol*. 2014;98(3):1001–1009. doi:10.1007/s00253-013-5422-8
14. Cioffi N, Ditaranto N, Torsi L, et al. Analytical characterization of bioactive fluoropolymer ultra-thin coatings modified by copper nanoparticles. *Anal Bioanal Chem*. 2005;381(3):607–616. doi:10.1007/s00216-004-2761-4
15. Bugata LSP, Venkata PP, Gundu AR, et al. Acute and subacute oral toxicity of copper oxide nanoparticles in female albino Wistar rats. *J Appl Toxicol*. 2019;39(5):702–716. doi:10.1002/jat.3760
16. Cholewińska E, Ognik K, Fotschki B, et al. Comparison of the effect of dietary copper nanoparticles and one copper (II) salt on the copper biodistribution and gastrointestinal and hepatic morphology and function in a rat model. *PLoS One*. 2018;13(5):e0197083. doi:10.1371/journal.pone.0197083
17. Zhang H, Chang Z, Mehmood K, et al. Nano copper induces apoptosis in PK-15 cells via a mitochondria-mediated pathway. *Biol Trace Elem Res*. 2018;181(1):62–70. doi:10.1007/s12011-017-1024-0
18. Tang H, Xu M, Shi F, et al. Effects and mechanism of nano-copper exposure on hepatic cytochrome P450 enzymes in rats. *Int J Mol Sci*. 2018;19(7):pii: E2140. doi:10.3390/ijms19072140
19. Singh CR, Kathiresan K, Anandhan S. A review on marine based nanoparticles and their potential applications. *Afr J Biotechnol*. 2015;14(18):1525–1532. doi:10.5897/AJB2015.14527
20. Sathiyavimal S, Vasantharaj S, Bharathi D, et al. Biogenesis of copper oxide nanoparticles (CuONPs) using *Sida acuta* and their incorporation over cotton fabrics to prevent the pathogenicity of Gram negative and Gram positive bacteria. *J Photochem Photobiol B*. 2018;188:126–134. doi:10.1016/j.jphotobiol.2018.09.014
21. Rahman A, Ismail A, Jumbianti D, et al. Synthesis of copper oxide nanoparticles by using Phormiiumcyanobacterium. *Indo J Chem*. 2009;9(3):355–360. doi:10.22146/ijc.21498
22. Pugazhendhi A, Prabakar D, Jacob JM, et al. Synthesis and characterization of silver nanoparticles using *Gelidium amansii* and its antimicrobial property against various pathogenic bacteria. *Microb Pathog*. 2018;114:41–45. doi:10.1016/j.micpath.2017.11.013
23. Crookes-Goodson WJ, Slocik JM, Naik RR. Bio-directed synthesis and assembly of nanomaterials. *Chem Soc Rev*. 2008;37:2403–2412.
24. Gade AK, Bonde P, Ingle AP, et al. Exploitation of aspergillus niger for synthesis of silver nanoparticles. *J Biobased Mater Bioenergy*. 2008;2(3):243–247. doi:10.1166/jbmb.2008.401
25. Lee HJ, Lee G, Jang NR, et al. Biological synthesis of copper nanoparticles using plant extract. *NSTI-Nanotech*. 2011;1:371–374.
26. Taylor WR. Marine algae of the eastern tropical and subtropical coasts of the America. *Univ Michigan Stud Sci Series*. 1985;21:825.
27. Abboud Y, Saffaj T, Chagraoui A, et al. Biosynthesis, characterization and antimicrobial activity of copper oxide nanoparticles (CONPs) produced using brown alga extract (*Bifurcariabifurcata*). *ApplNanosci*. 2014;4:571–576. doi:10.1007/s13204-013-0233-x
28. Khan A, Rashid A, Younas R, et al. A chemical reduction approach to the synthesis of copper nanoparticles. *Int Nano Lett*. 2016;6(1):21–26. doi:10.1007/s40089-015-0163-6
29. Sharma R, Bisen DP, Shukla U, et al. X-ray diffraction: a powerful method of characterizing nanomaterials. *Recent Res Sci Technol*. 2012;4(8):77–79.
30. Theivasanthi T, Alagar M. X-ray diffraction studies of copper nanopowder. *Arch Phys Res*. 2010;1(2):112–117.
31. Chen Z, Meng H, Xing G, et al. Acute toxicological effects of copper nanoparticles in vivo. *Toxicol Lett*. 2006;163(2):109–120. doi:10.1016/j.toxlet.2005.10.003
32. Reitman S, Frankel S. A colorimetric method for the determination of serum glutamic oxalacetic and glutamic pyruvic transaminases. *Am J Clin Pathol*. 1957;28(1):56–63. doi:10.1093/ajcp/28.1.56
33. Fawcett JK, Scott JE. A rapid and precise method for the determination of urea. *J. Clin. Path*. 1960;13(2):156–159. doi:10.1136/jcp.13.2.156
34. Schirmeister J. Determination of creatinine level. *Dtsch Med Wschr*. 1964;89:1940–1947.
35. Duran EM, Shapshak JP, Worle A, et al. Presenilin-1 detection in brain neurons and FOXP3 in peripheral blood mononuclear cells: normalizer gene selection for real time reverse transcriptase pcr using the deltadeltaCt method. *Front. Biosci*. 2005;10(1–3):2955–2965. doi:10.2741/1751
36. Georgopoulos G, Roy A, Yonone-Lioy MJ, et al. Environmental copper: its dynamics and human exposure issues. *J Toxicol Environ Health B Crit Rev*. 2001;4(4):341–394. doi:10.1080/10937401753146207
37. Siddiqi KS, Husen A. Fabrication of metal and metal oxide nanoparticles by algae and their toxic effects. *Nanoscale Res Lett*. 2016;11(1):363. doi:10.1186/s11671-016-1580-9
38. Askari S, Halladj R. Effects of ultrasound-related variables on sonochemically synthesized SAPO-34 nanoparticles. *J Solid State Chem*. 2013;201:85–92. doi:10.1016/j.jssc.2013.02.026
39. Alqadi M, Noqtah OA, Alzoubi F, et al. pH effect on the aggregation of silver nanoparticles synthesized by chemical reduction. *Mater Sci Poland*. 2014;32(1):107–111. doi:10.2478/s13536-013-0166-9
40. Betancourt-Galindo R, Reyes-Rodriguez PY, Puente-Urbina BA, et al. Synthesis of copper nanoparticles by thermal decomposition and their antimicrobial properties. *J Nano Arch*. 2014;10:1–5.
41. Pramila-Devamani RH, Sivakami S. Synthesis and characterization of copper chromate nanoparticles. *Weekly Sci Res J*. 2014;1:1–10.
42. Smith B. *Infrared Spectral Interpretation*. New York: CRC Press. Taylor & Francis Group; 1999.
43. Khalef WK. Preparation and characterization of Teo2 nano particles by pulsed laser ablation in water. *J Eng Technol*. 2014;32:396.
44. Castro L, Blázquez ML, Muñoz JA, et al. Biological synthesis of metallic nanoparticles using algae. *IET Nanobiotechnol*. 2013;7(3):109–116. doi:10.1049/iet-nbt.2012.0041
45. Chen LJ, Li GS, Li LP. CuONanocrystals in thermal decomposition of ammonium perchlorate. *J Therm Anal Calorim*. 2008;91(2):581–587. doi:10.1007/s10973-007-8496-7
46. Yedurkar SM, Maurya CB, Mahanwar PA. A biological approach for the synthesis of copper oxide nanoparticles by *ixora coccinea* leaf extract. *J Mater Environ Sci*. 2017;8:1173–1178.
47. Ortolani EL, Antonelli AC, Sarkis SJE. Acute sheep poisoning from a copper sulfate foot bath. *Vet Human Toxicol*. 2004;46:315–318.
48. Patel KC, Kulkarni BS, Acharya VN. Acute renal failure and methaemoglobinaemia due to copper sulphate poisoning. *J Postgrad Med*. 1976;22(4):180–184.
49. Gary D. *Osweiler. Toxicology. The National Veterinary Medical Series (NVMS)*. 1 ed. Wiley-Blackwell; 1996.
50. George LW, Carlson GP. Copper toxicosis. In: Smith BP, editor. *Large Animal Internal Medicine*. 3rd ed. St. Louis, MO: Mosby; 2002:1061–1062.
51. Nussey G, Vuren JHJ, Preez HH. Effect of copper on the differential white blood cell counts of the Mozambique tilapia (*Oreochromismossambicus*). *Comp Biochem Physiol C Pharmacol Toxicol Endocrinol*. 1995;111(3):381–388.lee.
52. Sarhan OMM, Hussein RM. Effects of intraperitoneally injected silver nanoparticles on histological structures and blood parameters in the albino rat. *Int J Nanomedicine*. 2014;9:1505–1517. doi:10.2147/IJN.S56729
53. Ebaid R, Elhussainy E, El-Shourbagy S, et al. Protective effect of Arthrospiraplatensis against liver injury induced by copper nanoparticles. *Orient Pharm Exp Med*. 2017;17(3):203–210. doi:10.1007/s13596-017-0264-z
54. Maddinedi SB. Green synthesis of Au–Cu_{2-x}Se heterodimer nanoparticles and their in-vitro cytotoxicity, photothermal assay. *Environ Toxicol Pharmacol*. 2017;53:29–33. doi:10.1016/j.etap.2017.05.006

55. Sarkar A, Das J, Manna P, et al. Nano-copper induces oxidative stress and apoptosis in kidney via both extrinsic and intrinsic pathways. *Toxicology*. 2011;290(2–3):208–217. doi:10.1016/j.tox.2011.09.086
56. Sizova E, Miroshnikov S, Polyakova V, et al. Copper nanoparticles as modulators of apoptosis and structural changes in tissues. *J Biomater Nanobiotechnol*. 2012;3(01):97–104. doi:10.4236/jbnb.2012.31013
57. Fahmy B, Cormier SA. Copper oxide nanoparticles induce oxidative stress and cytotoxicity in airway epithelial cells. *Toxicol Vitro*. 2009;23(7):1365–1371. doi:10.1016/j.tiv.2009.08.005
58. Ghosh M, Pal S, Sil PC. Taurine attenuates nano-copper-induced oxidative hepatic damage via mitochondria-dependent and NF-κB/TNF-α-mediated pathway, *Toxicol. Res*. 2014;3:474.
59. Galitsky VA. The Emergence of Eukaryotic Cells and the Origin of Apoptosis. *Cytology*. 2005;47(2):103–108.
60. Lei R, Wu C, Yang B, et al. Integrated metabolomic analysis of the nano sized copper particle-induced hepatotoxicity and nephrotoxicity in rats: a rapid in vivo screening method for nanotoxicity. *Toxicol Appl Pharmacol*. 2008;232(2):292–301. doi:10.1016/j.taap.2008.06.026
61. Meng H, Chen Z, Xing G, et al. Ultrahigh reactivity provokes nanotoxicity: explanation of oral toxicity of nano-copper particles. *Toxicol.Lett*. 2007;175(1–3):102–110. doi:10.1016/j.toxlet.2007.09.015
62. Privalova LI, Katsnelson BK, Loginova NV, et al. Subchronic toxicity of copper oxide nanoparticles and its attenuation with the help of a combination of bioprotectors. *Int. J. Mol. Sci*. 2014;15(7):12379–12406. doi:10.3390/ijms150712379
63. Mortazavi F, Javid AJ. Acute renal failure due to copper sulfate poisoning. *Iran J Pediatr*. 2009;19(1).
64. Oberdörster G, Oberdörster E, Oberdörster J. Nanotoxicology: an emerging discipline evolving from studies of ultrafine particles. *Environ Health Perspect*. 2005;113(7):823–839. doi:10.1289/ehp.7339
65. Lee IC, Ko JW, Park SH, et al. Comparative toxicity and biodistribution assessments in rats following subchronic oral exposure to copper nanoparticles and microparticles. *Part Fibre Toxicol*. 2016;13(1):56. doi:10.1186/s12989-016-0169-x
66. Mortimer M, Kasemets K, Kahru A. Toxicity of ZnO and CuO nanoparticles to ciliated protozoa Tetrahymenathermophila. *Toxicology*. 2010;269(2–3):182–189. doi:10.1016/j.tox.2009.07.007